Electronic Supplementary Information

for

Structural and Dynamical Aspects of Alkylammonium Salts of a Silicodecatungstate as Heterogeneous Epoxidation Catalysts

Sayaka Uchida,[a,b] Keigo Kamata,[a] Yoshiyuki Ogasawara,[a] Megumi Fujita,[a] and Noritaka Mizuno*[a]

[a]Department of Applied Chemistry, School of Engineering, The University of Tokyo, 7-3-1 Hongo, Bunkyo-ku, Tokyo 113-8656, Japan. Fax:+81-3-5841-7220; E-mail: tmizuno@mail.ecc.u-tokyo.ac.jp

[b]Present Address: Department of Basic Sciences, School of Arts and Sciences, The University of Tokyo, 3-8-1 Komaba, Meguro-ku, Tokyo 153-8902, Japan.

Materials. Substrates and solvents were purified according to the reported procedure.[S1] H_2O_2 (30% aqueous solution, Kanto Chemical) and deuterated solvents (CD_3CN, $CDCl_3$, and D_2O) were purchased from ACROS or Aldrich and used as received.

Syntheses of alkylammonium salts.

$[(CH_3)_4N]_4[\gamma\text{-SiW}_{10}O_{34}(H_2O)_2]$ **[C1]:** The tetramethylammonium salt was synthesized according to the literature procedure.[S2] Yield 4.2 g (70%) based on $K_8[\gamma\text{-SiW}_{10}O_{36}]\cdot 12H_2O$ (6.0 g). IR(KBr), 1000, 957, 918, 894, 872, 780, 710, 637, 599, 566, and 544 cm^{-1}; elemental analysis calcd (%) for $C_{16}H_{68}N_4O_{44}SiW_{10}$ ($[(CH_3)_4N]_4[\gamma\text{-SiW}_{10}O_{34}(H_2O)_2]\cdot 8H_2O$), C 6.66, H 2.37, N 1.94, Si 0.97, W 63.67; found, C 6.63, H 2.36, N 1.98, Si 0.93, W 63.33.

$[(n\text{-}C_3H_7)_4N]_4[\gamma\text{-SiW}_{10}O_{34}(H_2O)_2]$ **[C3]**: The tetra-*n*-propylammonium salt was synthesized according to the literature procedure;[S3] tetra-*n*-butylammonium bromide $[(n\text{-}C_4H_9)_4N]\cdot Br$ was replaced by tetra-*n*-propylammonium bromide $[(n\text{-}C_3H_7)_4N]\cdot Br$. Yield 4.6 g (48%) based on $K_8[\gamma\text{-SiW}_{10}O_{36}]\cdot 12H_2O$ (9.0 g). IR (KBr), 997, 957, 920, 904, 876, 784, 748, 700, 599, 565, and 543 cm^{-1}; elemental analysis calcd (%) for $C_{48}H_{120}N_4O_{38}SiW_{10}$ ($[(n\text{-}C_3H_7)_4N]_4[\gamma\text{-SiW}_{10}O_{34}(H_2O)_2]\cdot 2H_2O$), C 17.86, H 3.75, N 1.74, Si 0.87, W 56.95; found, C 18.06, H 3.66, N 1.76, Si 0.89, W 56.52.

$[(n\text{-}C_4H_9)_4N]_4[\gamma\text{-SiW}_{10}O_{34}(H_2O)_2]$ **[C4]**: The tetra-*n*-butylammonium salt was synthesized according to the literature procedure.[S2,S3] Yield 3.4 g (54%) based on $K_8[\gamma\text{-SiW}_{10}O_{36}]\cdot 12H_2O$ (6.0 g). IR (KBr), 999, 958, 920, 902, 877, 784, 745, 691, 565, and 544 cm^{-1}; elemental analysis calcd (%) for $C_{64}H_{150}N_4O_{37}SiW_{10}$ ($[(n\text{-}C_4H_9)_4N]_4[\gamma\text{-SiW}_{10}O_{34}(H_2O)_2]\cdot H_2O$), C 22.38, H 4.40, N 1.63, Si 0.82, W 53.53;

found, C 22.27, H 4.44, N 1.57, Si 0.80, W 53.24.

$[(n\text{-}C_5H_{11})_4N]_4[\gamma\text{-}SiW_{10}O_{34}(H_2O)_2]$ [**C5**]: The tetra-*n*-pentylammonium salt was synthesized according to the literature procedure;[S3] tetra-*n*-butylammonium $[(n\text{-}C_4H_9)_4N]^+$ was replaced by the aqueous solution of tetra-*n*-pentylammonium bromide $[(n\text{-}C_5H_{11})_4N]\cdot Br$. Yield 1.22 g (84%) based on $K_8[\gamma\text{-}SiW_{10}O_{36}]\cdot 12H_2O$ (1.2 g). IR (KBr), 997, 957, 923, 880, 832, 782, 737, 692, 656, 566, and 543 cm^{-1}; elemental analysis calcd (%) for $C_{80}H_{182}N_4O_{37}SiW_{10}$ ($[(n\text{-}C_5H_{11})_4N]_4[\gamma\text{-}SiW_{10}O_{34}(H_2O)_2]\cdot H_2O$), C 26.26, H 5.01, N 1.53, Si 0.77, W 50.25; found, C 26.14, H 5.05, N 1.58, Si 0.75, W 50.22.

Instruments. IR spectra were measured on a Jasco FT/IR-460 spectrometer Plus using KBr disks. NMR spectra were recorded on a JEOL JNM-EX-270 spectrometer (^1H, 270.0 MHz and ^{13}C, 67.80 MHz) by using 5 mm tubes. Chemical shifts (δ) were reported in ppm downfield from $Si(CH_3)_4$ (solvent, $CDCl_3$). ICP-AES analyses were performed with a Shimadzu ICPS-8100 spectrometer. GC analysis was carried out on Shimadzu GC-2014 with a flame ionization detector equipped with a DB-WAX etr capillary column (internal diameter = 0.25 mm, length = 30 m), an InertCap-5 capillary column (internal diameter = 0.25 mm, length = 30 m), or a TC-1 capillary column (internal diameter = 0.25 mm, length = 30 m). Mass spectra were recorded on a Shimadzu GCMS-QP2010 equipped with a TC-5HT capillary column at an ionization voltage of 70 eV.

A Typical Procedure for Catalytic Epoxidation of Alkenes with H_2O_2. Catalytic epoxidation of alkenes was carried out in a 30 mL glass vessel containing a magnetic stir bar. Epoxidation of propene and 1-butene was carried out with an autoclave having a Teflon vessel. The products were identified by comparison of their GC retention time, mass spectra, and ^1H and ^{13}C NMR spectra with the literature data.

References

[S1] *Purification of Laboratory Chemicals 3rd ed.* (Eds.: D. D. Perrin, W. L. F. Armarego), Pergamon Press, Oxford, **1988**.

[S2] K. Kamata, K. Yonehara, Y. Sumida, K. Yamaguchi, S. Hikichi, N. Mizuno, *Science*, **2003**, *300*, 964–966.

[S3] N. Mizuno, S. Uchida, K. Kamata, R. Ishimoto, S. Nojima, K. Yonehara, Y. Sumida, *Angew. Chem. Int. Ed.*, **2010**, *49*, 9972–9976.

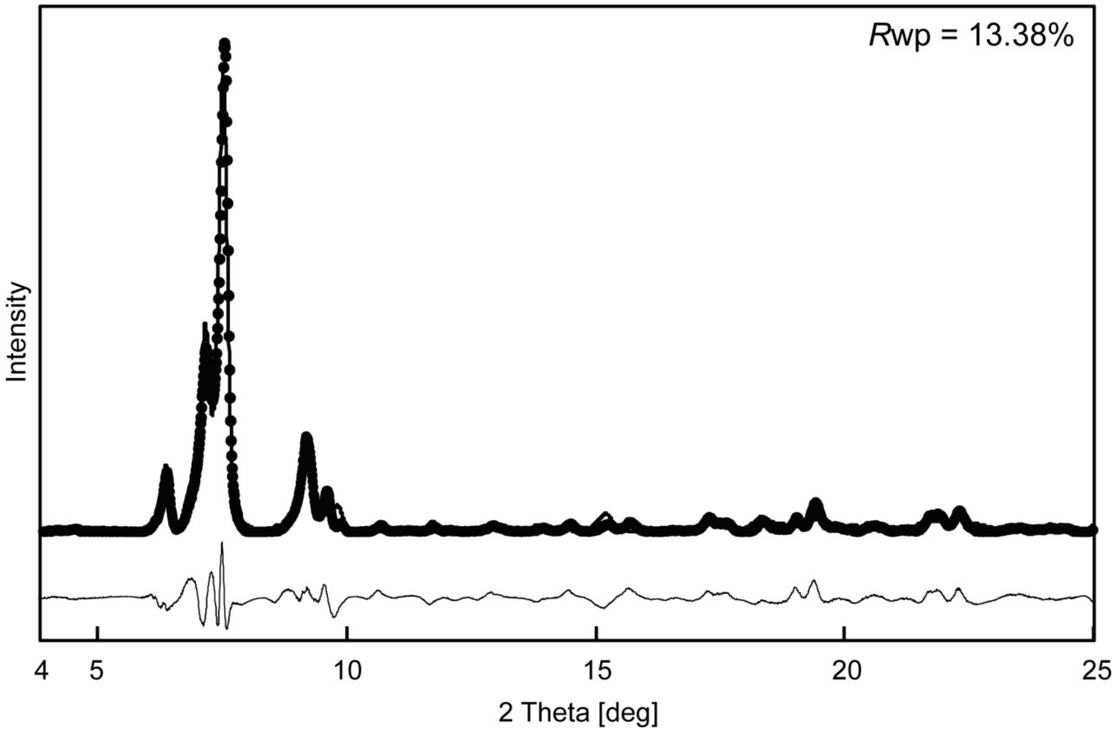

Fig. S1 Powder XRD pattern and result of Rietveld analysis of **C3**. Solid circles and solid line showed the experimental and calculated data, respectively. Solid line under the pattern showed the difference plot.

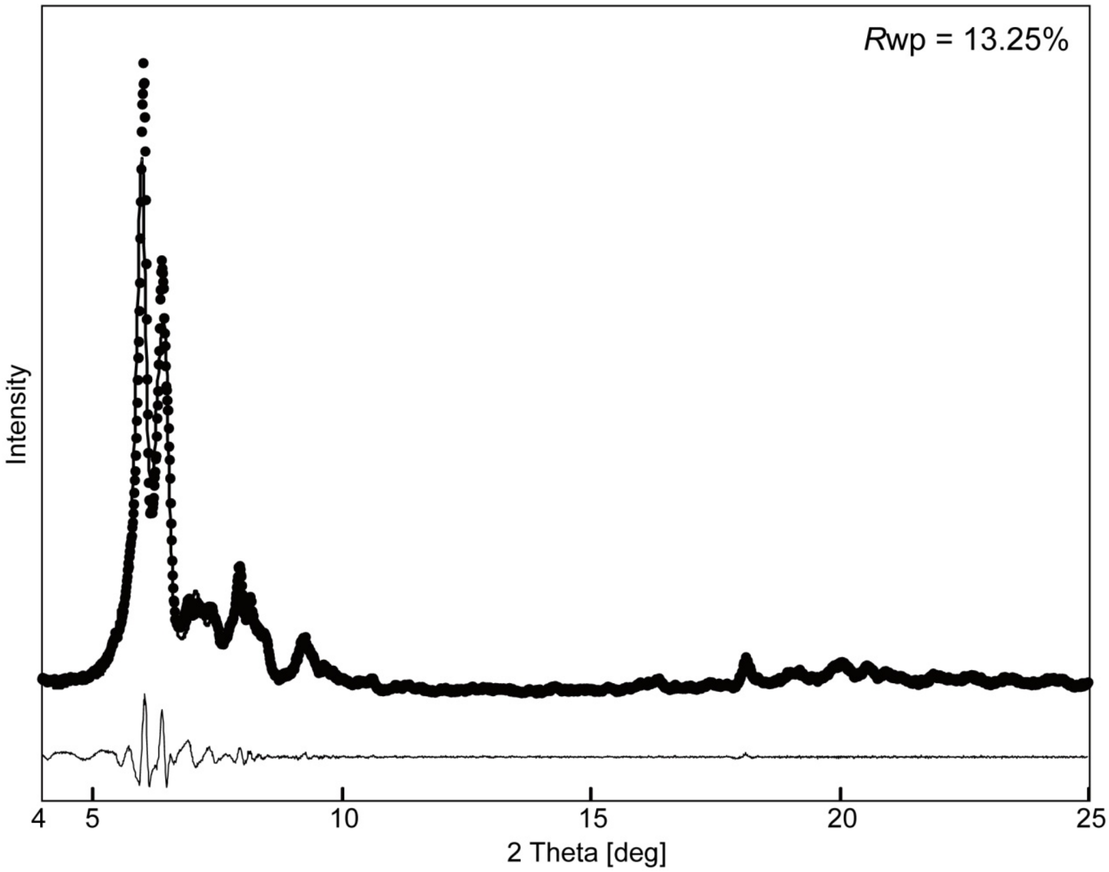

Fig. S2 Powder XRD pattern and result of Rietveld analysis of **C5**. Solid circles and solid line showed the experimental and calculated data, respectively. Solid line under the pattern showed the difference plot.

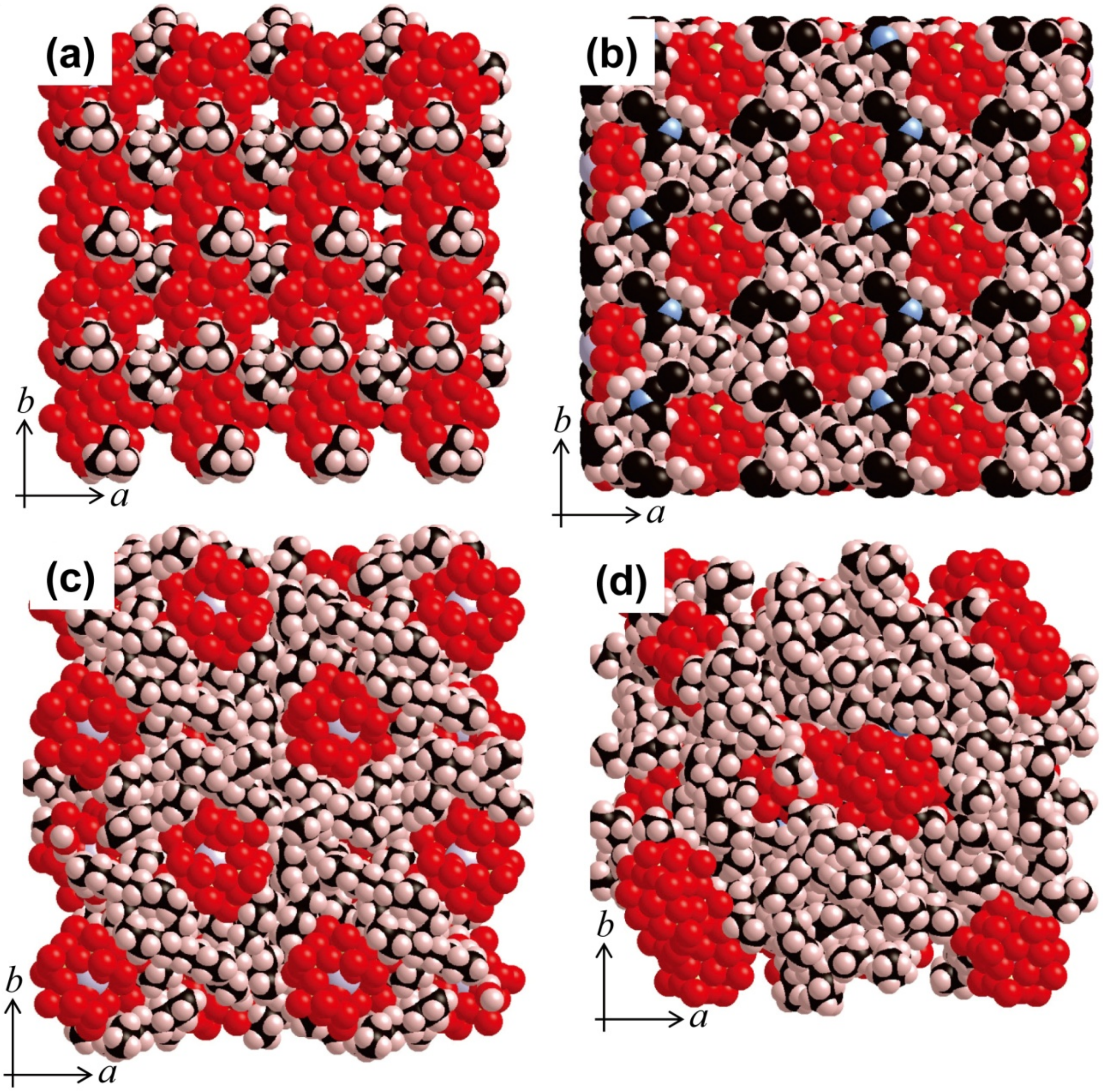

Fig. S3 Space filling models of the crystal structure of alkylammonium salts. (a) **C1**, (b) **C3**, (c) **C4**, and (d) **C5**. Red, light purple, light green, black, pink, and light blue spheres showed the oxygen (*r* = 1.5 Å), silicon (*r* = 2.1 Å), tungsten (*r* = 1.0 Å), carbon (*r* = 1.7 Å), hydrogen (*r* = 1.2 Å), and nitrogen (*r* = 1.5 Å) atoms, respectively. The figures in parenthesis showed the van der Waals radius for each atom (ref. A. Bondi, *J. Phys. Chem.* 1964, **68**, 441).

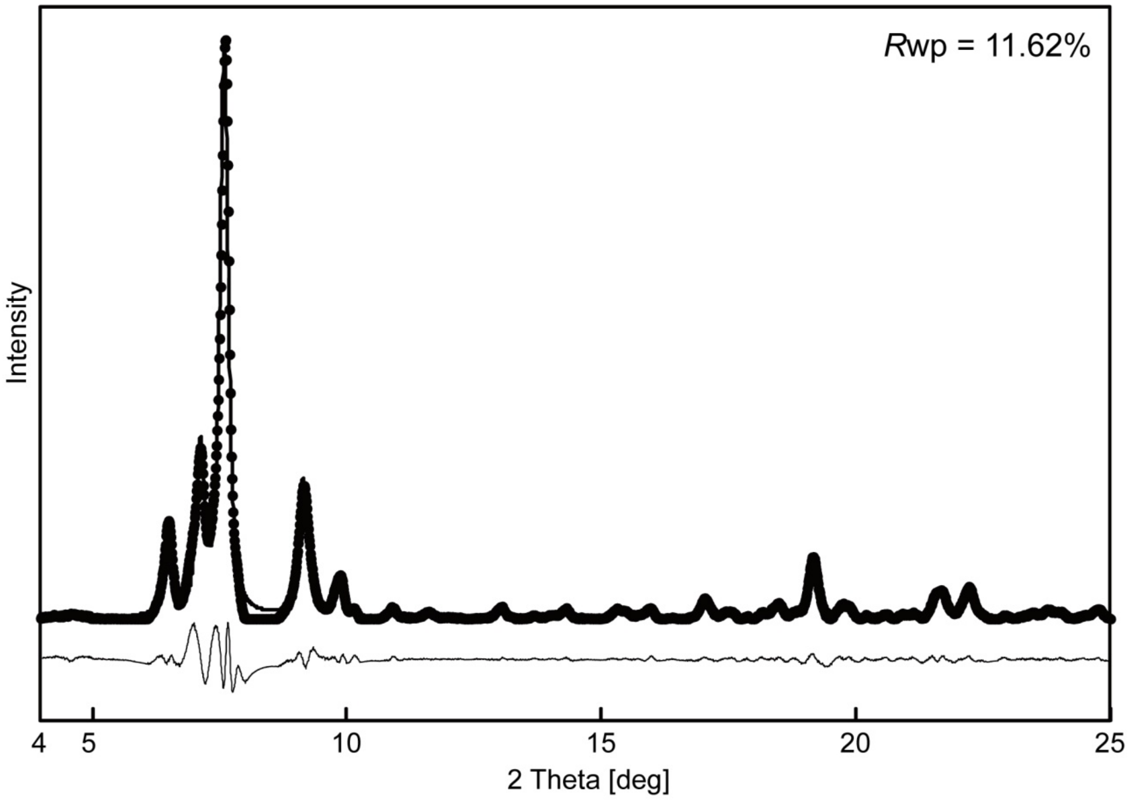

Fig. S4 Powder XRD pattern and result of Pawley analysis of **C3•0.5EtOAc**. Solid circles and solid line showed the experimental and calculated data, respectively. Solid line under the pattern showed the difference plot.

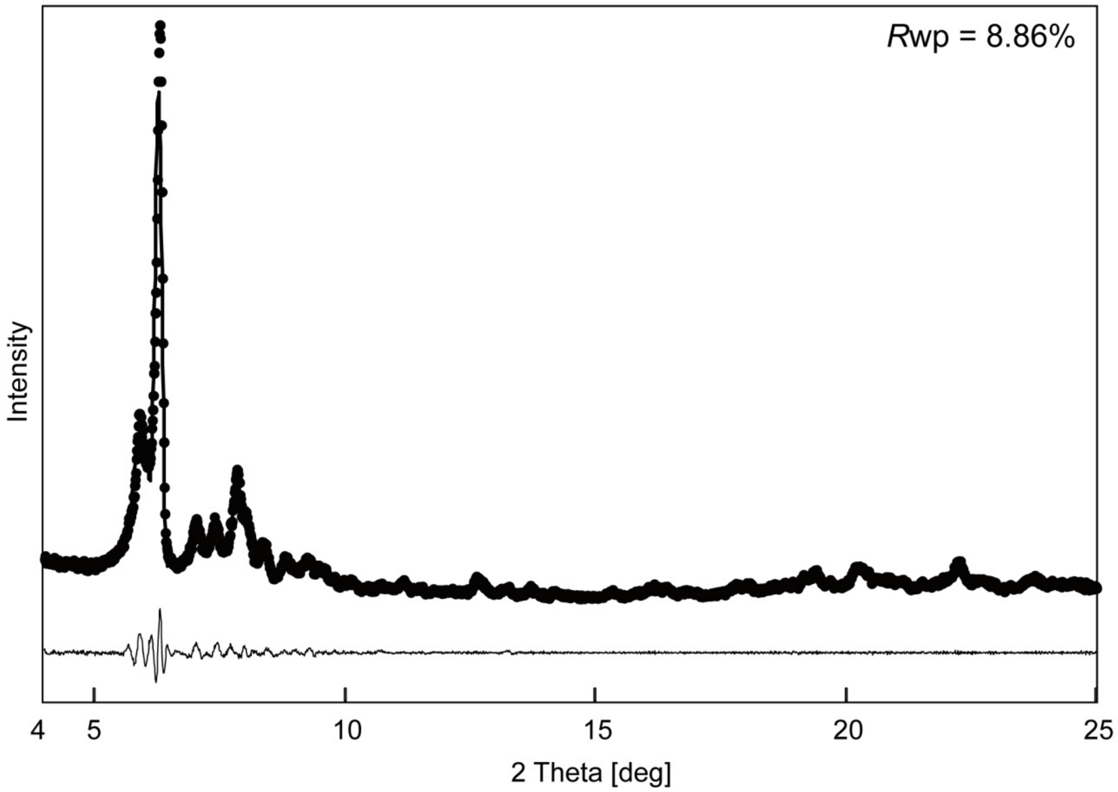

Fig. S5 Powder XRD pattern and result of Pawley analysis of **C5•EtOAc**. Solid circles and solid line showed the experimental and calculated data, respectively. Solid line under the pattern showed the difference plot.

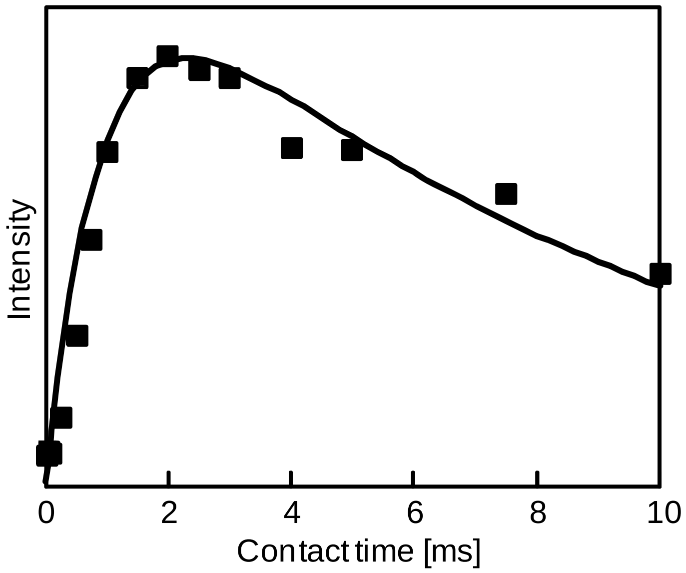

Fig. S6 Intensities of the C1 carbon signal of ^{13}C-CPMASNMR spectra of **C1** at 298 K as function of contact times. Square symbols and solid line showed the experimental and calculated data according to eq. (1), respectively.

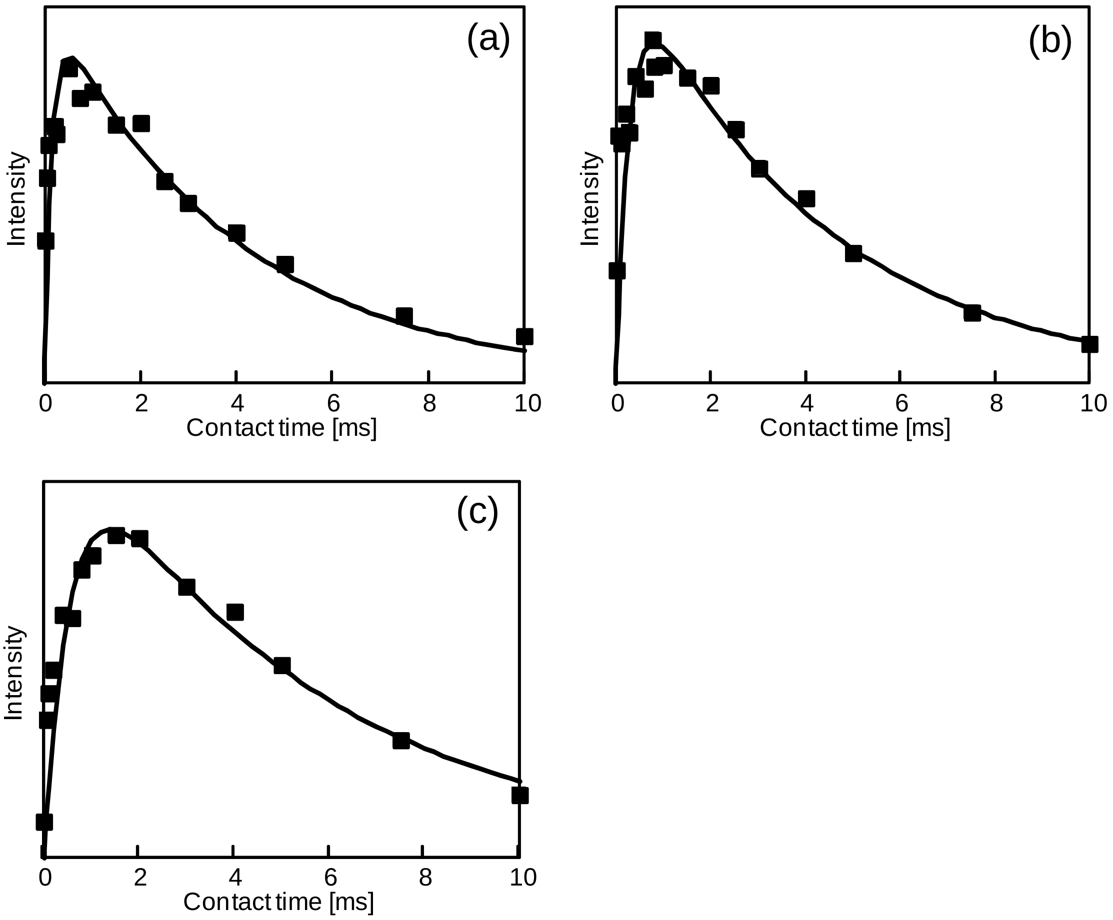

Fig. S7 Intensities of the signals of ^{13}C-CPMASNMR spectra of **C3** at 298 K as function of contact times. (a) C1 carbon (59.3 ppm), (b) C2 carbon (16.1 ppm), and (c) C3 carbon (11.3 ppm). Square symbols and solid lines showed the experimental and calculated data according to eq. (1), respectively.

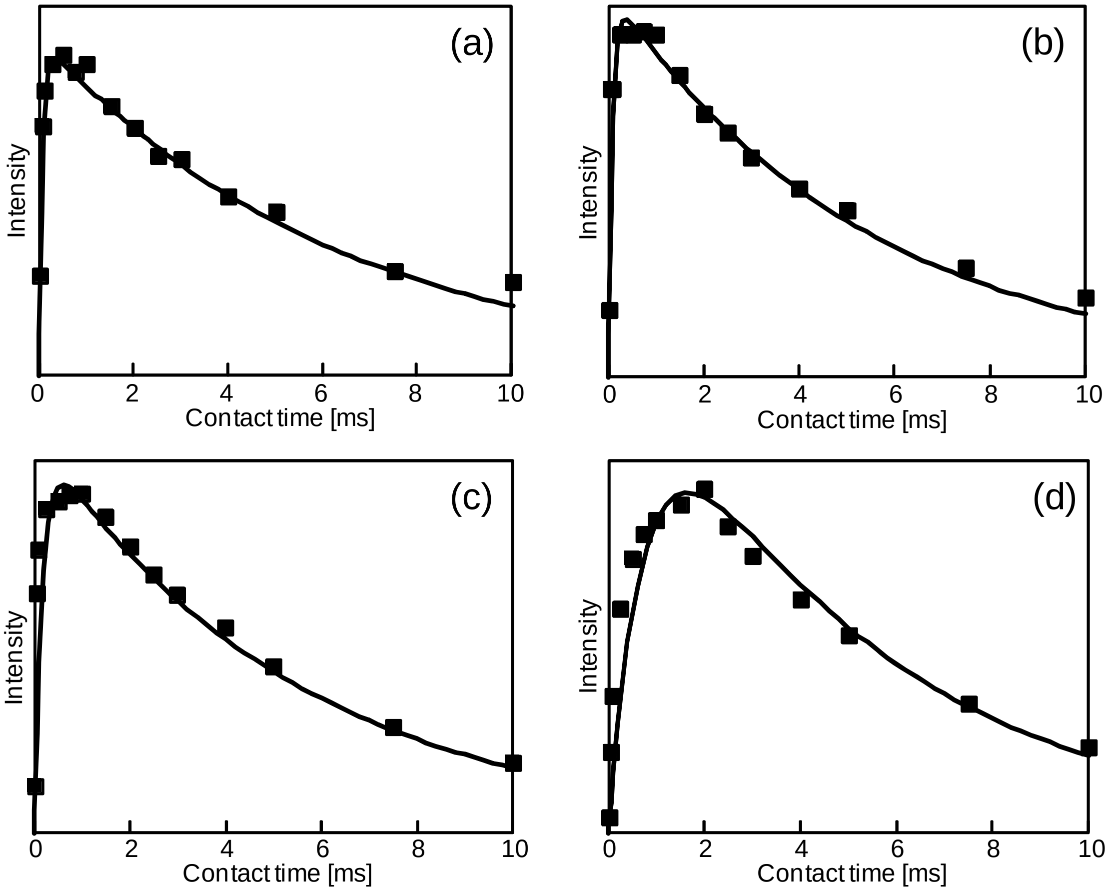

Fig. S8 Intensities of the signals of ^{13}C-CPMASNMR spectra of **C4** at 298 K as function of contact times. (a) C1 carbon (57.9 ppm), (b) C2 carbon (24.6 ppm), (c) C3 carbon (20.3 ppm), and (d) C4 carbon (14.9 ppm). Square symbols and solid lines showed the experimental and calculated data according to eq. (1), respectively.

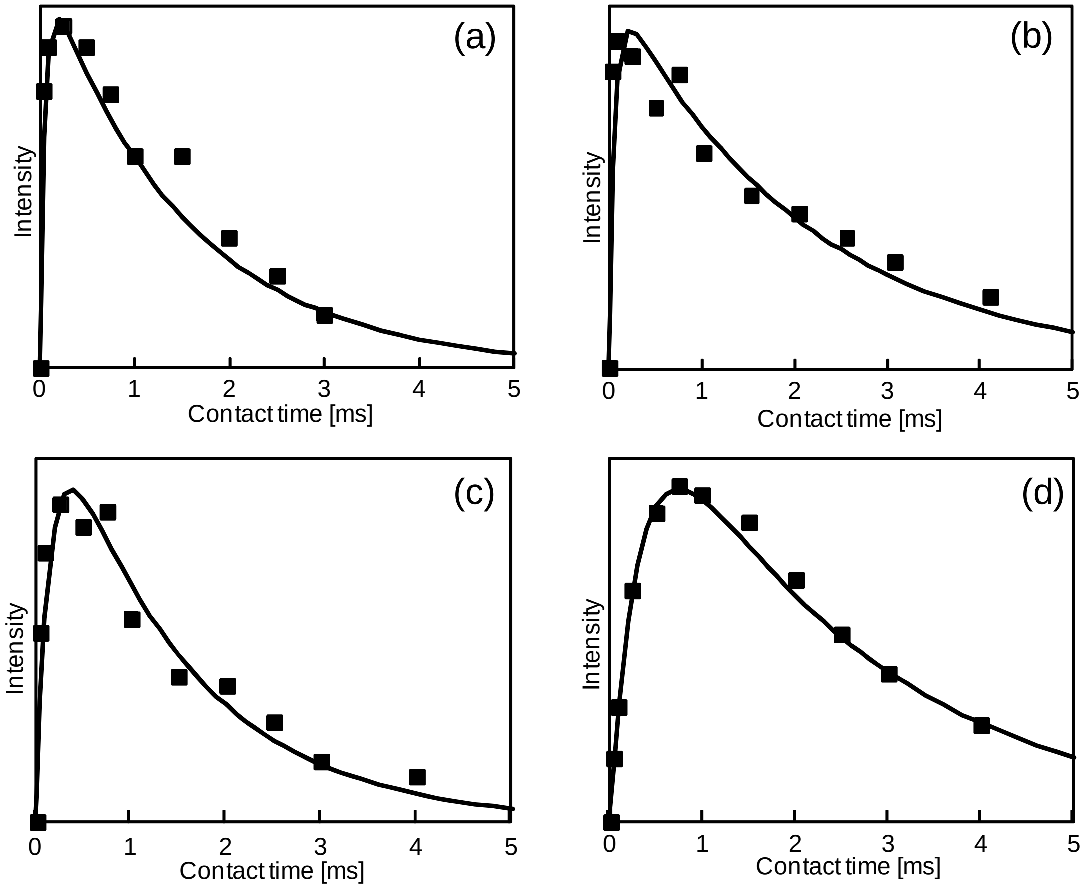

Fig. S9 Intensities of the signals of ^{13}C-CPMASNMR spectra of **C4•EtOAc** at 298 K as function of contact times. (a) C1 carbon (57.9 ppm), (b) C2 carbon (24.6 ppm), (c) C3 carbon (20.3 ppm), and (d) C4 carbon (14.9 ppm). Square symbols and solid lines showed the experimental and calculated data according to eq. (1), respectively.

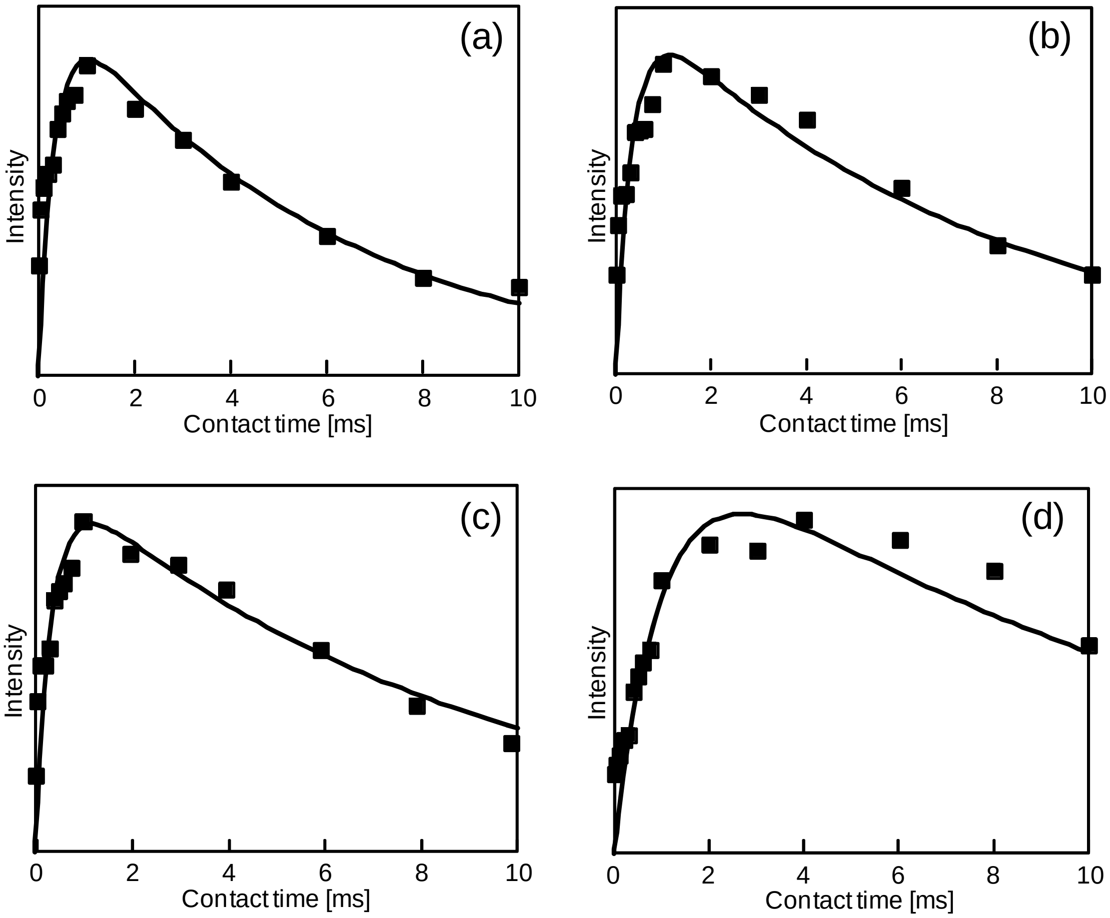

Fig. S10 Intensities of the signals of ^{13}C-CPMASNMR spectra of **C5** at 298 K as function of contact times. (a) C1 carbon (59.4 ppm), (b) C3 carbon (28.6 ppm), (c) C2 and C4 carbon (22.2 ppm), and (d) C5 carbon (13.8 ppm). Square symbols and solid lines showed the experimental and calculated data according to eq. (1), respectively.